

Resonant Terahertz Optical Sideband Generation from Confined Magnetoexcitons

J. Kono,^{1,*} M. Y. Su,² T. Inoshita,¹ T. Noda,³ M. S. Sherwin,² S. J. Allen, Jr.,² and H. Sakaki^{1,3}

¹*Quantum Transition Project, Japan Science and Technology Corporation, Tokyo 153, Japan*

²*Center for Terahertz Science and Technology and Department of Physics, University of California, Santa Barbara, California 93106*

³*Institute of Industrial Science, University of Tokyo, Tokyo 106, Japan*

(Received 20 March 1997)

We have probed the internal structure and nonlinear response of magnetoexcitons in GaAs/AlGaAs quantum wells by resonantly driving one- and two-photon internal transitions with intense terahertz electric fields. Strong near-band-gap emission lines, or optical sidebands, appear at frequencies $\omega_{\text{NIR}} \pm 2n\omega_{\text{THz}}$, where ω_{NIR} is the interband exciton-creation frequency, ω_{THz} is the frequency of the driving field, and n is an integer. The intensity of the sidebands exhibits pronounced enhancement when ω_{THz} coincides with transitions between magnetically tuned energy levels in the excitons, providing new and accurate information on the internal dynamics of excitons. [S0031-9007(97)03865-9]

PACS numbers: 78.20.Jq, 78.20.Ls, 78.66.-w

The dynamics of effective-mass particles and their complexes in an intense electric field strongly modifies the optical properties of a semiconductor in the vicinity of the absorption edge. In the well-known Franz-Keldysh effect, a strong dc electric field induces absorption below the edge [1] and oscillatory behavior of the absorption above the edge [2]. These electro-optical (EO) effects are well understood in many bulk and low-dimensional semiconductor systems [3]. Terahertz (THz) electric fields couple strongly with various elementary and collective intraband excitations in semiconductors, and we expect driven intraband excitations to significantly alter interband optical properties. Theoretical studies [4–6] have predicted fascinating new phenomena for the emission, absorption, and reflection properties of THz-driven semiconductors. Most notable is the ac Franz-Keldysh effect [4,6], which is predicted to be distinctly different from the dc versions.

Recently, a new type of two-color optical method for investigating THz resonances in semiconductors employing THz radiation and near infrared (NIR) or visible radiation has been developed [7–9]. When the THz radiation induces an *intraband* transition, the intensity of *interband* photoluminescence (PL) changes resonantly. This highly sensitive THz EO technique, optically detected THz resonance (ODTR) spectroscopy, has detected not only free-carrier cyclotron resonance (CR) but also a variety of THz resonances such as internal transitions of neutral and negatively charged donors [7] and excitons [8,9] in quantum wells (QW's).

In this Letter we report a very clear and dramatic THz EO effect. Incorporation of intense and coherent THz radiation in the above two-color scheme has resulted in a complete modification of the emission properties of undoped GaAs/AlGaAs QW's. We observed very strong NIR emission lines, or *sidebands* [10], at frequencies $\omega_{\text{NIR}} \pm 2n\omega_{\text{THz}}$, where ω_{NIR} (ω_{THz}) is the frequency of the NIR (THz) beam and n is an integer. The generation of the two-photon sideband is shown to be a third-order

nonlinear optical process involving one NIR photon and two THz photons, and is explained well in a theoretical model which treats both the NIR and THz fields as perturbations. The intensity of the sidebands exhibited pronounced resonances as a function of applied magnetic field. We attribute the resonances to virtual internal excitonic transitions. The results provide information on the internal structure and dynamics of confined excitons in unprecedented detail.

The sample consisted of 25 periods of undoped GaAs/Al_{0.3}Ga_{0.7}As (10 nm/15 nm) multiple QW's on 30 periods of GaAs/Al_{0.69}Ga_{0.31}As (4 nm/40 nm) etch-stop layers grown on a semiinsulating GaAs substrate. We selectively etched off the substrate, and measured the transmission spectrum with weak white light from a quartz-tungsten halogen lamp in order to determine the unperturbed energy levels at different magnetic fields.

For sideband generation, we employed a two-laser-beam setup, similar to what is usually used in ODTR spectroscopy [7–9], in a transmission geometry. Near-band-gap NIR radiation from a tunable cw Ti:sapphire laser passed through the sample, creating correlated electron-hole pairs, or excitons. The strong THz electric fields required for this experiment were provided by the UCSB Free-Electron Lasers, which are tunable between 4 and 160 cm⁻¹ (or 0.15 and 5 THz) and can attain peak powers of ~20 kW. The strong THz radiation passed through the sample collinearly with the NIR beam. The transmitted NIR radiation, consisting of the NIR fundamental, sidebands, and PL, was collected and sent to a monochromator-CCD camera combination via optical fiber. Magnetic fields up to 12 T were applied in the growth direction, parallel to both laser beams.

Figures 1(a) and 1(b) show typical sideband spectra at $B = 10$ T. The frequency of the THz radiation was 115 cm⁻¹ for both figures. In Fig. 1(a) NIR radiation resonantly creates the 2s heavy-hole (HH) excitons at 12 745 cm⁻¹. A strikingly narrow (width

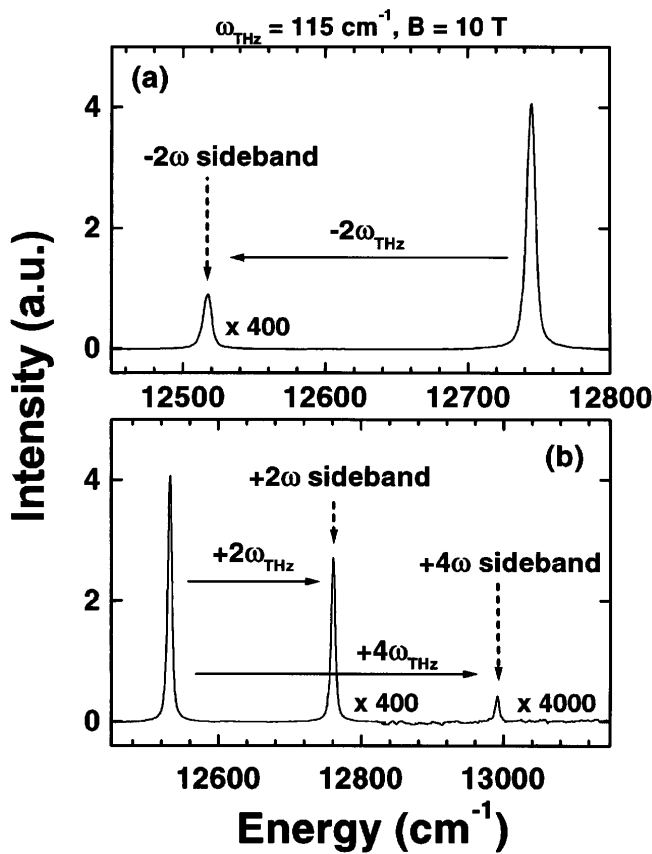


FIG. 1. Typical sideband generation spectra at $B = 10$ T. $\omega_{\text{THz}} = 115 \text{ cm}^{-1}$ for both figures. (a) Down conversion: $\omega_{\text{NIR}} = \omega_{2s} = 12745 \text{ cm}^{-1}$ and $\omega_{\text{sideband}} = \omega_{\text{NIR}} - 2\omega_{\text{THz}} = 12515 \text{ cm}^{-1}$. (b) Up conversion: $\omega_{\text{NIR}} = \omega_{1s} = 12515 \text{ cm}^{-1}$, $\omega_{\text{sideband}} = \omega_{\text{NIR}} + 2\omega_{\text{THz}} = 12745 \text{ cm}^{-1}$, and $\omega_{\text{NIR}} + 4\omega_{\text{THz}} = 12975 \text{ cm}^{-1}$.

$< 2 \text{ cm}^{-1}$) emission line, the -2ω sideband, is seen at *exactly* 12515 cm^{-1} [$= 12745 - (2 \times 115) \text{ cm}^{-1}$] only in the presence of THz radiation. In Fig. 1(b) the up-converted sidebands, the $+2\omega$ and $+4\omega$ sidebands, are seen above the NIR fundamental which resonantly excites the $1s$ HH excitons at 12531 cm^{-1} . The typical intensities of the -2ω , $+2\omega$, and $+4\omega$ sidebands are 0.05%, 0.15%, and 0.0015%, respectively, of the incident intensity of the fundamental, which was, in this case, about 100 mW/cm^2 . The $+4\omega$ sideband was observed only at the highest THz intensity ($\sim 10 \text{ kW/cm}^2$).

We studied the dependence of the intensity of the $+2\omega$ sideband on the powers of the incident NIR and THz beams at $B = 10$ T for $\omega_{\text{NIR}} = 12531 \text{ cm}^{-1}$ and $\omega_{\text{THz}} = 115 \text{ cm}^{-1}$. THz power was varied from 100 W to 1 kW, and NIR power from 0 to 1 W. We focused both laser beams on the same spot on the sample to ~ 1 mm. The intensity of the $+2\omega$ sideband increased *quadratically* with increasing THz power for a constant NIR power. For a constant THz power and low NIR power ($< 50 \text{ mW}$) the sideband intensity increased *linearly* with NIR power. At higher NIR powers we observed satu-

ration of the NIR power dependence. Thus at low NIR power the $+2\omega$ sideband emission can be described by a third-order nonlinear optical process involving one NIR photon and two THz photons. The same conclusion can be drawn for the -2ω sideband from power dependence studies, but we have not been able to perform systematic studies on the $+4\omega$ sideband because of its small intensity.

The sideband emission is strongly dependent on the polarization of the THz beam. We continuously changed the degree of circular polarization of the THz beam while monitoring the intensity of the $+2\omega$ sideband at $B = 10$ T for $\omega_{\text{NIR}} = 12531 \text{ cm}^{-1}$ and $\omega_{\text{THz}} = 115 \text{ cm}^{-1}$. The NIR laser beam was linearly polarized. The sideband intensity was strongest when the THz radiation was linearly polarized (parallel to the NIR polarization), decreased with increasing degree of circular polarization, and became weakest ($\sim 30\%$ of the strongest) when the THz radiation was circularly polarized. This strongly suggests that in order to produce the $+2\omega$ sideband there must be both right (σ^+ or electron-CR-active) and left (σ^- or electron-CR-inactive) circularly polarized THz radiation.

In Fig. 2 the $+2\omega$ sideband intensity is plotted vs B for $\omega_{\text{THz}} = 115 \text{ cm}^{-1}$ with $\omega_{\text{NIR}} = \omega_{1s}$ at all magnetic fields, where ω_{1s} is the creation frequency for $1s$ HH

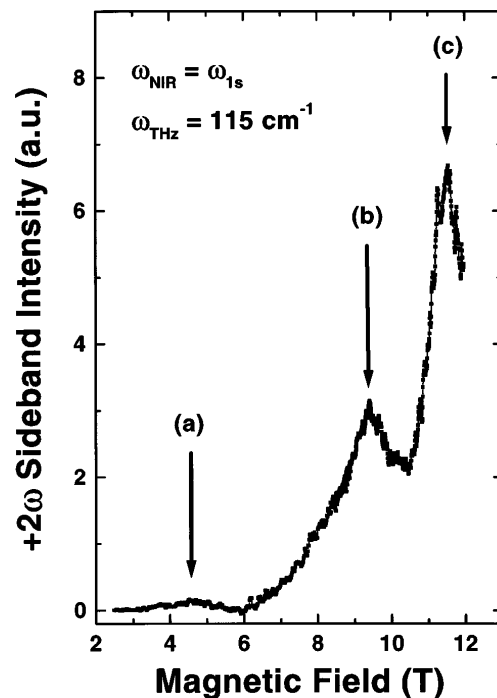


FIG. 2. The magnetic field dependence of the $+2\omega$ sideband intensity for $\omega_{\text{THz}} = 115 \text{ cm}^{-1}$ and $\omega_{\text{NIR}} = \omega_{1s}$ at all magnetic fields. The data demonstrate *nonlinear* optically detected THz resonances. Pronounced resonances occur when (a) $\omega_{\text{THz}} = \omega_{2p+} - \omega_{1s}$, (b) $2\omega_{\text{THz}} = \omega_{2s} - \omega_{1s}$, and (c) $\omega_{\text{THz}} = \omega_{2p-} - \omega_{1s}$. Note that the two-photon resonance (b) is forbidden in linear ODTR.

excitons. The data demonstrate novel *nonlinear* optically detected THz resonances. There are three distinct resonances at 4.5, 9.5, and 11.5 T, labeled as (a), (b), and (c), respectively. These resonances occur when (a) $\omega_{\text{THz}} = \omega_{2p+} - \omega_{1s}$, (b) $2\omega_{\text{THz}} = \omega_{2s} - \omega_{1s}$, and (c) $\omega_{\text{THz}} = \omega_{2p-} - \omega_{1s}$, in the low-field 2D hydrogenic notation. The resonance positions are in excellent agreement with those expected from linear ODTR experiments [8,9] and theory [11] on magnetoexcitons in 10-nm-wide GaAs QW's. Note that the two-photon resonance (b) is forbidden in linear ODTR.

We also studied in detail how the intensity of the $\pm 2\omega$ sidebands vary with ω_{NIR} at a constant magnetic field. We found that the sideband intensity is resonantly enhanced whenever either ω_{NIR} or $\omega_{\text{NIR}} \pm 2\omega_{\text{THz}}$ is resonant with an interband exciton-creation frequency such as ω_{1s} and ω_{2s} . The strongest $+2\omega$ sideband was observed when we satisfied the double-resonance condition, $\omega_{\text{NIR}} = \omega_{1s}$ and $\omega_{\text{NIR}} + 2\omega_{\text{THz}} = \omega_{2s}$. Similarly, the strongest -2ω sideband was obtained when $\omega_{\text{NIR}} - 2\omega_{\text{THz}} = \omega_{1s}$ and $\omega_{\text{NIR}} = \omega_{2s}$. These resonance conditions are well explained within our perturbation theory, which will be discussed next.

The $\pm 2\omega$ sideband generation can be described in terms of a third-order nonlinear susceptibility $\chi_{ijkl}^{(3)}$ defined by $P_i(\omega_{\text{NIR}} \pm 2\omega_{\text{THz}}) = \sum_{jkl} \chi_{ijkl}^{(3)} E_j(\pm\omega_{\text{THz}}) E_k(\pm\omega_{\text{THz}}) E_l(\omega_{\text{NIR}})$. Here $\vec{P}(\omega)$ and $\vec{E}(\omega)$ are the Fourier components of the polarization $\vec{P}(t)$ and the photon electric field $\vec{E}(t)$, respectively. [$\vec{P}(t) = \sum_{\omega} \vec{P}(\omega) e^{-i\omega t}$, etc.] It is important to realize that while the process resonates with certain intraband and interband excitations, no excitations of the material system are created. Thus the sideband generation is a parametric process [12], i.e., the initial and final states of the material are identical. At $T = 0$, this is the vacuum state with no electron-hole pairs (the valence band is full and the conduction band is empty). Let us assume that the NIR radiation induces interband transitions (exciton creation) and the THz radiation intraband transitions (exciton internal transitions). Then, in the case of the $+2\omega$ sideband, the standard perturbation theory [13] with the exciton-photon interaction $-\vec{p} \cdot \vec{E}$ (\vec{p} is the exciton polarization operator) leads to the following expression for $\chi^{(3)}$:

$$\chi_{ijkl}^{(3)} = \frac{-N_{\text{well}}}{\hbar^3} \sum_{\alpha\beta\gamma} \frac{\langle 0|p_i|\gamma\rangle \langle \gamma|p_j|\beta\rangle \langle \beta|p_k|\alpha\rangle \langle \alpha|p_l|0\rangle}{(\omega_{\text{NIR}} + 2\omega_{\text{THz}} - \omega_{\gamma} - i\Gamma)(\omega_{\text{NIR}} + \omega_{\text{THz}} - \omega_{\beta} - i\Gamma)(\omega_{\text{NIR}} - \omega_{\alpha} + i\Gamma)} + (\text{nonresonant terms}). \quad (1)$$

(The expression for the -2ω sideband is obtained by simply replacing ω_{THz} by $-\omega_{\text{THz}}$.) Here N_{well} is the well layer density; α , β , and γ run over the exciton states; $\omega_{\alpha} = (E_{\alpha} - E_0)/\hbar$ where $E_{\alpha}(E_0)$ is the energy of the exciton state $|\alpha\rangle$ (vacuum state $|0\rangle$); and Γ is a phenomenological damping factor. Numerical evaluation of Eq. (1) gives very large $\chi^{(3)} \sim 10^{-6}$ (10^{-3}) esu for off (on) resonance for $\Gamma \sim 1$ meV. If we treat the exciton in the spherical approximation, its state can be specified by using the 2D hydrogenic notation ($1s$, $2s$, $2p\pm$, $3s$, $3p\pm$, etc.). Then symmetry requires that α and γ in Eq. (1) be s states and β be a p state.

Equation (1) indicates that $\chi^{(3)}$ is resonantly enhanced when (A) $\omega_{\text{NIR}} = \omega_{ns}$, (B) $\omega_{\text{NIR}} + \omega_{\text{THz}} = \omega_{n'pm}$ ($m = \pm 1$), or (C) $\omega_{\text{NIR}} + 2\omega_{\text{THz}} = \omega_{n''s}$. These resonance conditions agree with the experimental observations and can be well visualized by using the diagrams shown in Figs. 3(a)–3(c). Here the dashed lines are the intermediate *virtual* levels [14] that exist only when the material system is interacting with the laser fields, whereas the solid lines are *real* magnetoexcitonic levels such as $|1s\rangle$, $|2s\rangle$, and $|2p\pm\rangle$. If one of the real levels is nearly coincident with one of the virtual levels, resonant enhancement of $\chi^{(3)}$ occurs. In all the three cases (a)–(c), two of the above three conditions (A)–(C) are satisfied:

(a) $\omega_{\text{NIR}} = \omega_{1s}$, $\omega_{\text{NIR}} + \omega_{\text{THz}} = \omega_{2p+}$, (b) $\omega_{\text{NIR}} = \omega_{1s}$, $\omega_{\text{NIR}} + 2\omega_{\text{THz}} = \omega_{2s}$, and (c) $\omega_{\text{NIR}} = \omega_{1s}$, $\omega_{\text{NIR}} + \omega_{\text{THz}} = \omega_{2p-}$. In (b) [(c)] the detuning of the remaining unsatisfied condition $\Delta = (\omega_{\text{NIR}} + \omega_{\text{THz}}) - \omega_{2p-}$ [$(\omega_{\text{NIR}} + 2\omega_{\text{THz}}) - \omega_{2s}$] is also small (less than 10 cm^{-1}), consistent with the observed large peaks (see Fig. 2). On the other hand, the large detuning

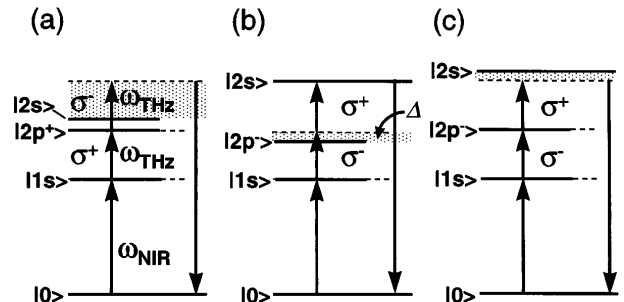


FIG. 3. Diagrammatic representation of the resonant processes responsible for the observed three resonances in Fig. 2. The dashed lines represent virtual levels, whereas the solid lines represent real magnetoexcitonic levels. Resonances occur when real levels coincide with virtual levels. The shaded area represents the magnitude of the detuning Δ .

($>100\text{ cm}^{-1}$) in (a) results in the small peak intensity as seen in Fig. 2.

Equation (1) also explains the polarization dependence of the sideband intensity. Let us consider the case where $|\alpha\rangle = |1s\rangle$, $|\beta\rangle = |2p-\rangle$, and $|\gamma\rangle = |2s\rangle$. If the THz radiation is left circularly polarized (σ^-), it can induce the $1s \rightarrow 2p-$ transition, but then it cannot induce the subsequent $2p- \rightarrow 2s$ transition due to angular momentum conservation, leading to vanishing sideband intensity. Similarly, for a THz photon of the opposite helicity (σ^+), the first transition is forbidden while the second is allowed. On the other hand, the sideband intensity is maximum for linearly polarized THz radiation, which is an equal-weight mixture of circular polarizations of opposite helicities, consistent with the experimental results [15].

In summary, we report the observation of strong near-band-gap emission lines, or optical sidebands, in undoped GaAs/AlGaAs QW's at high magnetic fields. We have shown that the sideband generation is due to the THz nonlinear dynamics of confined excitons. We conclude that the present two-color optical experiment conducted in conjunction with the theoretical scheme presented above is a sensitive and powerful tool for probing the nonlinear dynamics of quantum-confined carriers driven by strong ac THz electric fields.

This work was supported by ONR N00014-K-0692, QUEST DMR91-20007, and JST Quantum Transition Project. The authors are grateful to T. Ando, G. E. W. Bauer, A. B. Dzyubenko, A. Imamoglu, and K. Johnsen for useful comments and discussions, and D. P. Enyeart, D. T. White, and J. R. Allen at the Center for Terahertz Science and Technology for technical support.

*Visiting scientist at the University of California, Center for Terahertz Science and Technology, Santa Barbara, California 93106.
Electronic address: kono@qi.ucsb.edu

- [1] W. Franz, Z. Naturforsch. **13**, 484 (1958); L. V. Keldysh, Zh. Eksp. Teor. Fiz. **34**, 1138 (1958) [Sov. Phys. JETP **7**, 788 (1958)].
- [2] J. Callaway, Phys. Rev. **130**, 549 (1963).
- [3] See, e.g., *Semiconductors and Semimetals*, edited by R. K. Willardson and A. C. Beer (Academic Press, New York, 1972), Vol. 9; M. Cardona, *Modulation Spectroscopy, Solid State Physics* (Academic Press, New York, 1969), Suppl. 11; S. Schmitt-Rink, D. S. Chemla, and D. A. B. Miller, Adv. Phys. **38**, 89 (1989); S. Schmeller, W. Hansen, J. P. Kotthaus, G. Trankle, and G. Weimann, Appl. Phys. Lett. **64**, 330 (1994).
- [4] Y. Yacoby, Phys. Rev. **169**, 610 (1968).
- [5] T. Meier, F. Rossi, P. Thomas, and S. W. Koch, Phys. Rev. Lett. **75**, 2558 (1995).
- [6] A. P. Jauho and K. Johnsen, Phys. Rev. Lett. **76**, 4576 (1996).
- [7] J. Kono, S. T. Lee, M. S. Salib, G. S. Herold, A. Petrou, and B. D. McCombe, Phys. Rev. B **52**, R8654 (1995), and references therein.
- [8] J. Černe, J. Kono, M. S. Sherwin, M. Sundaram, A. C. Gossard, and G. E. W. Bauer, Phys. Rev. Lett. **77**, 1131 (1996).
- [9] M. S. Salib, H. A. Nickel, G. S. Herold, A. Petrou, B. D. McCombe, R. Chen, K. K. Bajaj, and W. Schaff, Phys. Rev. Lett. **77**, 1135 (1996).
- [10] Preliminary results can be found in J. Kono, J. Černe, T. Inoshita, M. S. Sherwin, M. Sundaram, and A. C. Gossard, in *Proceedings of 23rd International Conference on the Physics of Semiconductors*, edited by M. Scheffler and R. Zimmermann (World Scientific, Singapore, 1996), p. 1911; see also J. Černe *et al.*, Appl. Phys. Lett. **70**, 3543 (1997).
- [11] G. E. W. Bauer and T. Ando, Phys. Rev. B **38**, 6015 (1988).
- [12] For definition, see, e.g., R. W. Boyd, *Nonlinear Optics* (Academic Press, New York, 1992), p. 14.
- [13] Y. R. Shen, *The Principles of Non-linear Optics* (John Wiley & Sons, Inc., New York, 1984), Chap. 2.
- [14] For definition, see, e.g., Ref. [12], p. 5.
- [15] This polarization dependence is only approximate since the valence band mixing makes the excitons anisotropic.